

Mechanical properties of nerve roots and rami radicales isolated from fresh pig spinal cords

Norihiro Nishida^{1,*}, Tsukasa Kanchiku¹, Junji Ohgi², Kazuhiko Ichihara³, Xian Chen⁴, Toshihiko Taguchi⁵

1 Department of Orthopedic Surgery, Yamaguchi University Graduate School of Medicine, Yamaguchi, Japan

2 Faculty of Engineering, Yamaguchi University, Yamaguchi, Japan

3 Non-Profit Organization Corporation, Japan Orthopedic Biomechanics Institute, Yamaguchi, Japan

4 Faculties of Engineering, Yamaguchi University, Yamaguchi, Japan

5 Department of Orthopedic Surgery, Yamaguchi University Graduate School of Medicine, Yamaguchi, Japan

*Correspondence to:

Norihiro Nishida, M.D.,
nishida3@yamaguchi-u.ac.jp

orcid:

0000-0001-7754-6579 (Norihiro Nishida)

doi: 10.4103/1673-5374.170319

<http://www.nrronline.org/>

Accepted: 2015-08-10

Abstract

No reports have described experiments designed to determine the strength characteristics of spinal nerve roots and rami radicales for the purpose of explaining the complexity of symptoms of medullary cone lesions and cauda equina syndrome. In this study, to explain the pathogenesis of cauda equina syndrome, monoaxial tensile tests were performed to determine the strength characteristics of spinal nerve roots and rami radicales, and analysis was conducted to evaluate the stress-strain relationship and strength characteristics. Using the same tensile test device, the nerve root and ramus radicales isolated from the spinal cords of pigs were subjected to the tensile test and stress relaxation test at load strain rates of 0.1, 1, 10, and 100 s⁻¹ under identical settings. The tensile strength of the nerve root was not rate dependent, while the ramus radicales tensile strength tended to decrease as the strain rate increased. These findings provide important insights into cauda equina symptoms, radiculopathy, and clinical symptoms of the medullary cone.

Key Words: nerve regeneration; cauda equina syndrome; monoaxial tensile tests; radiculopathy; strength characteristics; stress-strain relationship; lumbar spinal canal stenosis; paralysis; spinal cord; neural degeneration

Nishida N, Kanchiku T, Ohgi J, Ichihara K, Chen X, Taguchi T (2015) Mechanical properties of nerve roots and rami radicales isolated from fresh pig spinal cords. *Neural Regen Res* 10(11):1869-1873.

Introduction

The cauda equina consists of nerve roots of the second and subsequent lumbar nerves joining within the spinal canal. Cauda equina syndrome is caused by compressive lesions, such as disc hernia and trauma, presenting with dyskinesia, sensory disorders, and bladder and rectal disorders. Furthermore, compression due to lesions of the medullary cone can also cause symptoms of myelopathy. To clarify the pathophysiology of cauda equina syndrome, morphological and histological evaluations have been conducted, involving preparation of models of chronic nerve root compression, traction of nerve roots, and other techniques (Jancalek et al., 2007; Singh et al., 2015). To date, however, no reports have described experiments designed to determine the strength characteristics of nerve roots and rami radicales for the purpose of explaining the complexity of symptoms of medullary cone lesions and cauda equina syndrome.

In this study, we conducted a monoaxial tensile test using the nerve roots and rami radicales isolated from fresh pig spinal cords to analyze the stress-strain relationships and strength characteristics.

Materials and Methods

Tensile test machine

The same testing machine was used for all measurements in

this study. The speed and dislocation were set using a personal computer (Windows XP Home Edition, One Microsoft Way Redmond, WA 98052-7329, USA and BTO, Naniwa, Osaka, Japan), and the pulling rate was controlled with a servo controller (SRCD10+RGU-2 Yamaha; Iwata, Shizuoka, Japan). The mobile part attached to the actuator was driven by the servo motor (T9H 20BK-400 Yamaha; Iwata, Shizuoka, Japan). The data for dislocation of the mobile part were collected with the rotary encoder attached to the servo motor and fed through the encoder board (PCI-6204 Interface; Kyobashi, Minami, Hiroshima, Japan) into the personal computer. The load data for the test samples were collected with the load cell (LTS-100GA Kyowa; Cyofugaoka, Cyofu, Tokyo, Japan) and fed through a dynamic strain meter (DPM-700B Kyowa; Cyofugaoka, Cyofu, Tokyo, Japan) and an AD conversion board (PCI-3171A Interface; Kyobashi, Minami, Hiroshima, Japan) into the personal computer (Figure 1A, B).

The program for controlling the measurements with the testing device was prepared with Microsoft Visual Basic 6.0 (One Microsoft Way Redmond, WA 98052-7329, USA). This program was used for setting the conditions for measurement (sampling frequency, pulling rate, tensile dislocation, and *etc.*) and processing of the data.

Preparation of nerve root samples

Samples were collected from the spinal cords of two pigs

within 12 hours after slaughter for human consumption. Two pigs were hybrid (Landrace and Duroc), aged 13 months, weighing 120–130 kg, both genders (Ginchiku ranch company, Hofu, Yamaguchi, Japan). The pigs used in this experiment were dismantled for meat to eat. As confirmed by Science Research Center, Institute of Life Science and Medicine of Yamaguchi University, Japan, the precise procedure was unnecessary. The vertebral arch on the dorsal side of the spinal canal was resected with an electric saw (MJ-300, RYOBI) to expose the dura mater and the spinal cord (Figure 2A). The nerve root was then dissected at the level of the intervertebral foramen, and the medullary cone and nerve root were isolated from the spine while still wrapped with the dura mater (Figure 2B). The dura mater around the spinal cord and the nerve root were then resected (Figure 3A), and samples 1–4 were assigned to the nerve root sections (sample No. 1 was assigned to the nerve root section most proximal to the point of bifurcation). During this process, the dura mater at the end of the nerve root facing the intervertebral foramen was left partially unresected to enable subsequent fixation on the testing device. For a similar reason, the spinal cord tissue at the origin of the nerve root was left partially unresected (Figure 3B).

The sample was fixed in the testing device (Figure 1B) by pinching the central and peripheral sides of the nerve root between the upper and lower jigs. To prevent the sample from falling off, the sample was fixed by suturing with 4-0 looped nylon using the method of Tsuge (1977).

Preparation of ramus radicales samples

The specimens were immersed in physiological saline to enable ramus radicales samples to be prepared without dam-

aging the specimen (Figure 3B). The diameter of each ramus radicales sample was measured with a 3D laser microscope (LEXT OLS4000; Olympus, Japan), followed by calculation of the cross-sectional area. A mean cross-section of 0.069 mm² (range: 0.067–0.071 mm²) was adopted. To analyze the mechanical strength characteristics of the nerve roots and constituent rami radicales, samples were subjected to the tensile test and to the stress relaxation test at a gauge length of 10 mm and temperature of 25°C as reported earlier (Ichihara et al., 2001). The load strain rates were 0.1, 1, 10 and 100 s⁻¹ using 3, 4, 3 and 4 samples of nerve roots and 4, 6, 6, and 5 samples of ramus radicales, respectively. We used Microsoft Office Home and Business 2010 Excel (One Microsoft Way Redmond, WA 98052-7329, USA) for preparing figures.

Results

Nerve root tensile test results

To analyze the mechanical properties of nerve roots following compression by trauma or because of degeneration of the disc or vertebral body, we conducted tensile tests. Figure 4A shows the stress-strain relationships for nerve roots analyzed using monoaxial tensile tests. With each sample, the stress gradually increased towards its maximum as the strain increased, thus exhibiting a superelastic pattern. After reaching its maximum value, the stress began to decrease gradually even as the strain increased further.

Rate dependency of nerve root

To investigate damage to the nerve root caused by speed, we further evaluated the results of the tensile test. Figure 4B

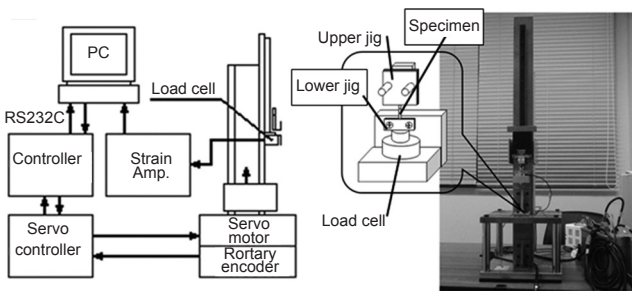


Figure 1 Experimental set up (A) and tensile test machine (B).

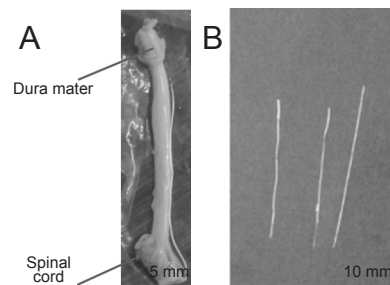


Figure 3 Nerve root and ramus radicales. (A) The dura mater around the spinal cord and the nerve root were resected. (B) The spinal cord tissue at the origin of the nerve root was left partially unresected.

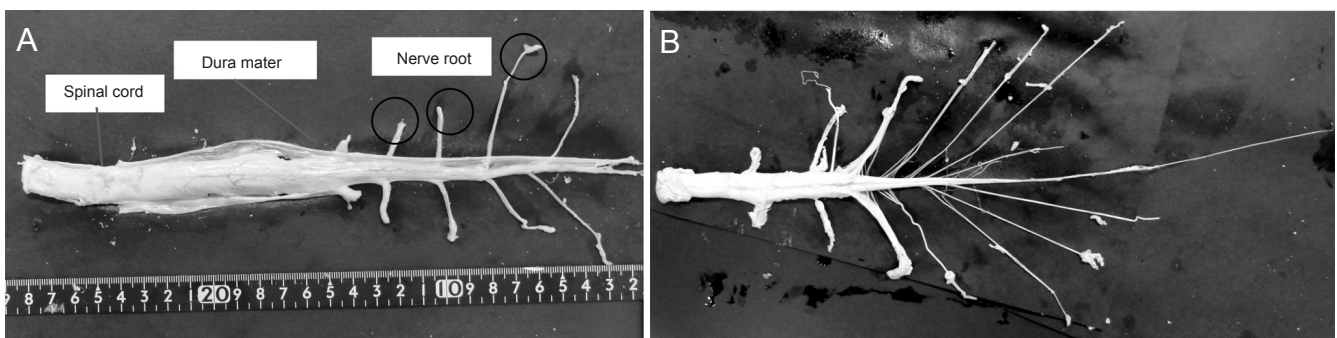


Figure 2 Anatomy of spine and nerve.

The dura mater, spinal cord and cauda (A). The nerve root was then dissected at the level of the intervertebral foramen, and the medullary cone and nerve root were isolated from the spine while still wrapped with the dura mater (B).

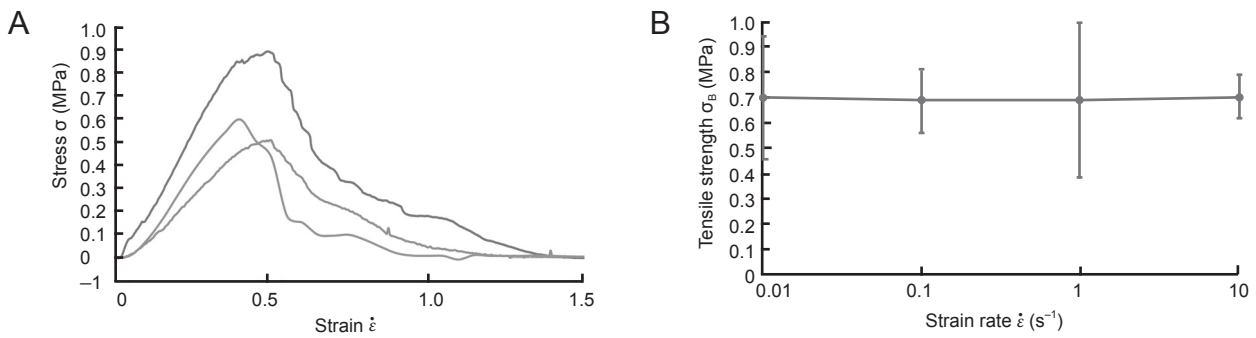


Figure 4 Nerve root tensile test results.

The stress-strain relationships for lumbar nerve roots as analyzed using monoaxial tensile tests (A). (B) The data for nerve root tensile strength (σ_B) in relation to the strain rate ($\dot{\epsilon}$).

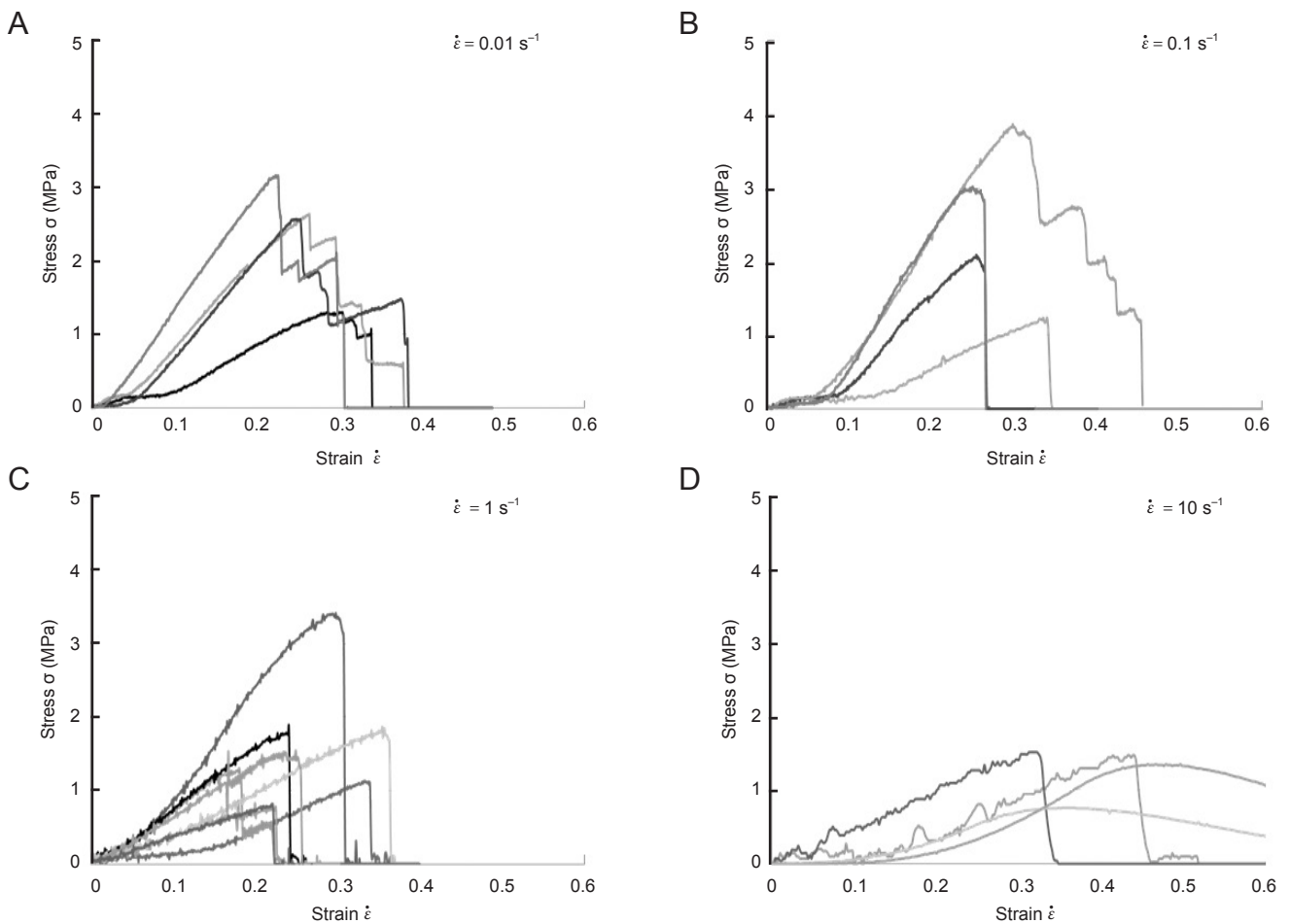


Figure 5 Analysis of stress-strain relationships based on ramus radicales samples.

(A) $\dot{\epsilon} = 0.01 s^{-1}$; (B) $\dot{\epsilon} = 0.1 s^{-1}$; (C) $\dot{\epsilon} = 1 s^{-1}$. (D) $\dot{\epsilon} = 10 s^{-1}$. The stress decreased in a stepwise manner after reaching a peak, with the decrease becoming more rapid as the strain rate increased.

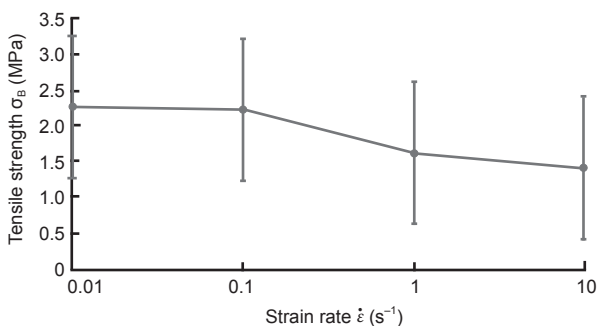


Figure 6 The data for the mean tensile strength (σ_B) of all ramus radicales samples in relation to the load strain rate ($\dot{\epsilon}$).

shows the data for nerve root tensile strength (σ_B) in relation to the load strain rate ($\dot{\epsilon}$). When $\dot{\epsilon} = 1.0 \text{ s}^{-1}$ the relationship between σ_B and $\dot{\epsilon}$ remained relatively constant, despite large variations in these parameters, and the tensile strength was not rate dependent. At each strain rate, the nerve root σ_B was approximately 0.7 MPa.

Ramus radicales tensile test results

To examine differences between the nerve root and ramus radicales, we conducted similar tensile tests to investigate the mechanical properties of ramus radicales. **Figure 5A–D** shows stress-strain relationships using ramus radicales samples. Although differences in $\dot{\epsilon}$ did not influence deformation patterns, the response to stress of the ramus radicales differed markedly to that of nerve roots. When $\dot{\epsilon} = 0.01 \text{ s}^{-1}$ the stress decreased in a stepwise manner after reaching a peak, with the decrease becoming more rapid as the strain rate increased.

Rate dependency of ramus radicales tensile strength

To examine the effect of speed on damage to the ramus radicales, we further evaluated the results of tensile testing. **Figure 6** shows results for the mean tensile strength (σ_B) of all ramus radicales samples in relation to the load strain rate ($\dot{\epsilon}$). The tensile strength of the ramus radicales tended to decrease as the load strain rate increased.

Discussion

The pathophysiology and classification of lumbar spinal canal stenosis were first reported by Arnoldi (1976). After this initial report, many researchers performed clinical and animal studies examining the symptoms of cauda equina in the context of blood flow (Ooi et al., 1990; Takahashi et al., 1993; Ikawa et al., 2005) and dural pressure both in the standing position and at rest (Takahashi et al., 1995a, b). According to these reports, the dural pressure during walking or in the standing position is approximately twice that in the supine position, and the disruption of circulation in patients with cauda equina syndrome is attributable to venous retention rather than to insufficient arterial blood supply.

Furthermore, for clarification of the pathophysiology of compressive radiculopathy, experiments on acute compression (Delamarter et al., 1990; Olmarker et al., 1991; Kobayashi et al., 1993) and chronic compression (Kobayashi et al., 2004a, b) have been carried out to evaluate nerve degeneration and pathological changes. In addition, evaluation of nerve root traction and compression has also been conducted frequently. Singh et al. (2015) reported that the morphological changes in nerve roots vary depending on the type of external force. Moreover, Jancalek et al. (2007) conducted histological evaluations of the internal structures of nerves exposed to external force. Reports have also described studies of molecules involved in pain, such as tumor necrosis factor (TNF)- α during nerve root compression (Obata et al., 2004; Sekiguchi et al., 2009). These experiments were designed to create a similar environment of entrapment neuropathy by applying a constant pressure to the nerve.

While previous reports have evaluated blood flow or pressure, histological features or degeneration, and the pathology/chemistry, no studies have examined the mechanical properties of nerve roots or rami radicales. When discussing the occurrence of paralysis arising from compression or trauma, mechanical properties also need to be taken into consideration. Although previous studies investigated the pathological and chemical changes of nerve roots following compression, they did not evaluate damage to the nerve caused by force and speed of injury. While this can be described with respect to future changes in the nerve, it is not possible to estimate the degree of nerve damage or to predict the effects of speed and traction. Our analysis is capable of shedding light on this. For example, after trauma to the thoracolumbar vertebral junction, symptoms are diverse because this area is governed by the upper and lower motor neurons of the spinal cord parenchyma, cauda equina, and nerve roots, thus making diagnosis difficult (Elsberg, 1996). The symptoms in these tissues may be associated with the strength characteristics of the cauda equina, in addition to the anatomical complexity and the manner of compression (Wall et al., 1990a, b). For these reasons, we attempted tensile tests to clarify the mechanical properties of these tissues.

A similar evaluation of the strength characteristics of nerves was previously reported by Ichihara et al. (2001) who analyzed the material characteristics of the spinal cord (gray and white matter). Based on data describing these mechanical properties, simulation by the finite element method has been conducted for analysis of the features of spinal cord disease, yielding results that were very similar to clinical knowledge (Kato et al., 2008, 2009, 2010; Nishida et al., 2011, 2012, 2013, 2014). In the present study, the nerve root tensile strength showed no rate dependency and was about 0.7 MPa; this value is 16 times the gray matter strength and 47 times the white matter strength reported by Ichihara et al. (2001). These results indicated that the nerve root has higher tensile strength than the spinal cord. This feature may be associated with the observation that severe injury of the nerve root in the medullary cone is unlikely to occur. Regarding the rami radicales, the present study suggested the possibility that the nerve may be injured suddenly when exposed to certain stress. As the pulling rate increased, the likelihood for injury tended to increase as well. Additionally, the stepwise decrease in stress in the nerve root, unlike that in the ramus radicales, seemed to be attributable to the composite structure of the nerve root, which is comprised of multiple rami, connective tissue, and fat tissue.

Since it is difficult to acquire human nerve root or ramus radicales for study, we used tissues from the pig as an alternative. Clinical symptoms of cauda equina, radiculopathy and the medullary cone can be evaluated in relation to results obtained with the finite element method. If the finite element method analyses based on the mechanical properties of pig tissues correlate with the clinical symptoms of the patient, this may help to understand the underlying pathology and therefore help to choose the best therapeutic strategy.

This study had a few limitations. First, we did not perform

evaluation of blood flow. Additionally, the pig specimens may have undergone histological degeneration during the 12-hour period from collection to examination. However, the finding that the nerve roots and rami radicales had higher strength than the spinal cord may be important for analyzing the medullary cone and cauda equina and for understanding the clinical symptoms of diseases involving this areas.

Taken together, we performed tensile load tests in nerve roots and rami radicales. The tensile strength of nerve roots was not rate dependent, while the tensile strength of rami radicales tended to decrease as the strain rate increased. Our data showed that nerve roots and rami radicales exhibited higher strength than the gray and white matter of the spinal cord. These findings provide important insight into the clinical symptoms of cauda equina syndrome and of diseases associated with the nerve roots and medullary cone.

Acknowledgments: *Special thanks to Mr. Syota Tahara, Mr. Yoshitaka Kanda, Mr. Yuuta Haruna, Mr. Kunitaka Fukuda, Mr. Hidetaka Morita and Mr. Seiya Miyazaki who were cooperator and enforcer of the experiments.*

Author contributions: *NN and JO wrote the paper. JO and KI performed experiments. TK, XC, and TT guided the research. All authors approved the final version of this paper.*

Conflicts of interest: *None declared.*

Plagiarism check: *This paper was screened twice using Cross-Check to verify originality before publication.*

Peer review: *This paper was double-blinded, stringently reviewed by international expert reviewers.*

References

- Arnoldi CC, Brodsky AE, Cauchoix J, Crock HV, Dommissie GF, Edgar MA, Gargano FP, Jacobson RE, Kirkaldy-Willis WH, Kurihara A, Langenskiöld A, Macnab I, McIvor GW, Newman PH, Paine KW, Russin LA, Sheldon J, Tile M, Urist MR, Wilson WE, Wiltse LL (1976) Lumbar spinal stenosis and nerve root entrapment syndromes. Definition and classification. *Clin Orthop Relat Res* (115):4-5.
- Delamarter RB, Bohlman HH, Dodge LD, Biro C (1990) Experimental lumbar spinal stenosis. Analysis of the cortical evoked potentials, microvasculature, and histopathology. *J Bone Joint Surg Am* 72:110-120.
- Elsberg C (1996) Diagnosis and treatment of surgical disease of the spinal cord and its membranes. pp63-65. WB saunders, Philadelphia.
- Ichihara K, Taguchi T, Yoshinori S, Ituo S, Shunichi K, Shinya K (2001) Gray matter of the bovine cervical spinal cord is mechanically more rigid and fragile than the white matter. *J Neurotrauma* 18:361-367.
- Ikawa M, Atsuta Y, Tsunekawa H (2005) Ectopic firing due to artificial venous stasis in rat lumbar spinal canal stenosis model: a possible pathogenesis of neurogenic intermittent claudication. *Spine* 30:2393-2397.
- Jancalck R, Dubovy P (2007) An experimental animal model of spinal root compression syndrome: an analysis of morphological changes of myelinated axons during compression radiculopathy and after decompression. *Exp Brain Res* 179:111-119.
- Kato Y, Kanchiku T, Imajo Y, Ichihara K, Kawano S, Hamanaka D, Yaji K, Taguchi T (2009) Flexion model simulating spinal cord injury without radiographic abnormality in patients with ossification of the longitudinal ligament: the influence of flexion speed on the cervical spine. *J Spinal Cord Med* 32:555-559.
- Kato Y, Kanchiku T, Imajo Y, Kimura K, Ichihara K, Kawano S, Hamanaka D, Yaji K, Taguchi T (2010) Biomechanical study of the effect of the degree of static compression of the spinal cord in ossification of the posterior longitudinal ligament. *J Neurosurgery Spine* 12: 301-305.
- Kato Y, Kataoka H, Ichihara K, Imajo Y, Kojima T, Kawano S, Hamanaka D, Yaji K, Taguchi T (2008) Biomechanical study of cervical flexion myelopathy using a three-dimensional finite element method. *J Neurosurgery Spine* 8:436-441.
- Kobayashi S, Yoshizawa H, Yamada S (2004a) Pathology of lumbar nerve root compression. Part 1: Intraradicular inflammatory changes induced by mechanical compression. *J Orthop Res* 22:170-179.
- Kobayashi S, Yoshizawa H, Yamada S (2004b) Pathology of lumbar nerve root compression. Part 2: morphological and immunohistochemical changes of dorsal root ganglion. *J Orthop Res* 22:180-188.
- Kobayashi S, Yoshizawa H, Hachiya Y, Ukai T, Morita T (1993) Vasogenic edema induced by compression injury to the spinal nerve root. Distribution of intravenously injected protein tracers and gadolinium-enhanced magnetic resonance imaging. *Spine* 18:1410-1424.
- Nishida N, Kato Y, Imajo Y, Kawano S, Taguchi T (2011) Biomechanical study of the spinal cord in thoracic ossification of the posterior longitudinal ligament. *J Spinal Cord Med* 34:518-522.
- Nishida N, Kato Y, Imajo Y, Kawano S, Taguchi T (2012) Biomechanical analysis of cervical spondylotic myelopathy: The influence of dynamic factors and morphometry of the spinal cord. *J Spinal Cord Med* 35:256-261.
- Nishida N, Kanchiku T, Kato Y, Imajo Y, Kawano S, Taguchi T (2013) Biomechanical analysis of the spinal cord in Brown-Séquard syndrome. *Exp Ther Med* 6:1184-1188.
- Nishida N, Kanchiku T, Kato Y, Imajo Y, Yoshida Y, Kawano S, Taguchi T (2014) Biomechanical analysis of cervical myelopathy due to ossification of the posterior longitudinal ligament: effects of posterior decompression and kyphosis following decompression. *Exp Ther Med* 7:1095-1099.
- Obata K, Yamanaka H, Kobayashi K, Dai Y, Mizushima T, Katsura H, Fukuoka T, Tokunaga A, Noguchi K (2004) Role of mitogen-activated protein kinase activation in injured and intact primary afferent neurons for mechanical and heat hypersensitivity after spinal nerve ligation. *J Neurosci* 24:10211-10222.
- Olmarker K (1991) Spinal nerve root compression. Nutrition and function of the porcine cauda equina compressed in vivo. *Acta Orthop Scand Suppl* 242:1-27.
- Ooi Y, Mita F, Satoh Y (1990) Myeloscopic study on lumbar spinal canal stenosis with special reference to intermittent claudication. *Spine* 15:544-549.
- Sekiguchi M, Sekiguchi Y, Konno S, Kobayashi H, Homma Y, Kikuchi S (2009) Comparison of neuropathic pain and neuronal apoptosis following nerve root or spinal nerve compression. *Eur Spine J* 18:1978-1985.
- Singh J, Hussain F, Decuzzi P (2015) Role of differential adhesion in cell cluster evolution: from vasculogenesis to cancer metastasis. *Comput Methods Biomech Biomed Engin* 18:282-292.
- Takahashi K, Kagechika K, Takino T, Matsui T, Miyazaki T, Shima I (1995a) Changes in epidural pressure during walking in patients with lumbar spinal stenosis. *Spine* 20: 2746-2749.
- Takahashi K, Miyazaki T, Takino T, Matsui T, Tomita K (1995b) Epidural pressure measurements. Relationship between epidural pressure and posture in patients with lumbar spinal stenosis. *Spine* 20:650-653.
- Takahashi K, Olmarker K, Holm S, Porter RW, Rydevik B (1993) Double-level cauda equina compression: an experimental study with continuous monitoring of intraneural blood flow in the porcine cauda equina. *J Orthop Res* 11:104-109.
- Tsuge K, Yoshikazu I, Matsuishi Y (1977) Repair of flexor tendons by intratendinous tendon suture. *J Hand Surg Am* 2:436-440.
- Wall EJ, Cohen MS, Massie JB, Rydevik B, Garfin SR (1990a) Cauda equina anatomy. I: Intrathecal nerve root organization. *Spine* 15:1244-1247.
- Wall EJ, Cohen MS, Abitbol JJ, Garfin SR (1990b) Organization of intrathecal nerve roots at the level of the conus medullaris. *J Bone Joint Surg Am* 72:1495-1499.

Copypedited by Tang Z, Yang S, Li CH, Song LP, Zhao M